

PHYSICAL REVIEW LETTERS

VOLUME 85

11 SEPTEMBER 2000

NUMBER 11

Measurement of the Angular Momentum of a Rotating Bose-Einstein Condensate

F. Chevy, K. W. Madison, and J. Dalibard

Laboratoire Kastler Brossel Département de Physique de l'Ecole Normale Supérieure, 24 rue Lhomond, 75005 Paris, France
(Received 12 May 2000)

We study the quadrupole oscillation of a Bose-Einstein condensate of ^{87}Rb atoms confined in an axisymmetric magnetic trap, after it has been stirred by an auxiliary laser beam. The stirring may lead to the nucleation of one or more vortices, whose presence is revealed unambiguously by the precession of the axes of the quadrupolar mode. For a stirring frequency Ω below the single vortex nucleation threshold Ω_c , no measurable precession occurs. Just above Ω_c , the angular momentum deduced from the precession is $\sim \hbar$. For stirring frequencies above Ω_c the angular momentum is a smooth and increasing function of Ω , until an angular frequency is reached at which the vortex lattice disappears.

PACS numbers: 03.75.Fi, 32.80.Lg, 67.40.Db

The achievement of Bose-Einstein condensation in atomic gases has led to a new impulse in the study of quantum gases [1–4]. Among the many issues which can be investigated in these systems the properties of quantum vortices are some of the most intriguing and debated. A vortex is a singularity line around which the circulation of the velocity field is nonzero. For a superfluid this circulation is quantized and equal to nh/M , where n is an integer and M the atomic mass [5]. These quantized vortices play an essential role in macroscopic quantum phenomena, such as the superfluidity of liquid helium [6] or the response of a superconductor to an external magnetic field [7]. In this paper we determine the angular momentum of a gaseous Bose-Einstein condensate, as it is stirred near the vortex nucleation threshold. We show that the angular momentum per atom along the stirring axis, L_z , jumps from zero to \hbar (within experimental uncertainty). We also measure the increase of L_z as more vortices are nucleated in the system, for a stirring frequency higher than the nucleation threshold.

We consider here a condensate harmonically trapped in a quasicylindrically symmetric potential. The angular momentum of the condensate along the symmetry axis z of the trap is measured using the frequencies of its collective excitations. More precisely, as suggested in [8], we study the two transverse quadrupole modes carrying angular momentum along the z axis of $m = \pm 2$ (see also [9–11]). In the absence of vortices, the frequencies $\omega_{\pm}/2\pi$ of these

two modes are equal as a consequence of the reflection symmetry about the xy plane. By contrast, for $L_z \neq 0$, this degeneracy is lifted by an amount:

$$\omega_+ - \omega_- = 2L_z/(Mr_{\perp}^2), \quad (1)$$

where r_{\perp}^2 stands for the average value of $x^2 + y^2$ for the condensate. Consequently the measurements of $\omega_+ - \omega_-$ and of the transverse size of the condensate provide the angular momentum of the gas.

The result (1) is valid if the system is properly described by the hydrodynamic theory for superfluids [8]. This requires that the number of atoms N is much larger than the ratio a_{ho}/a , where a_{ho} is the size of the ground state of the transverse motion in the trap and a the scattering length describing the interactions between atoms at low temperature. For our experimental conditions the quantity Na/a_{ho} is larger than 1000 which ensures the validity of (1). The prediction (1) can be interpreted in terms of the Sagnac effect: in the presence of a vortex the condensate rotates and this lifts the degeneracy of the two excitations $m = \pm 2$.

Two experiments have led so far to the observation of a vortex line in a gaseous condensate [12,13]. The method used in [12] uses a combination of a laser and a microwave field to print the desired velocity field onto the atomic wave function. This generates a condensate with atoms in a given internal state rotating around a second, stationary condensate in another internal state. The second method

[13], which is used in the present paper, is a transposition of the rotating bucket experiment performed on ^4He . We superimpose onto the cylindrically symmetric magnetic potential a nonaxisymmetric, dipole potential created by a stirring laser beam. The combined potential leads to a cigar-shaped harmonic trap with a slight anisotropic transverse profile. The transverse anisotropy is rotated at an angular frequency Ω and nucleates a vortex if above a critical frequency Ω_c .

The details of the experimental setup have been described in [13,14]. For the preparation of the condensate we start with 10^9 ^{87}Rb atoms in a Ioffe-Pritchard magnetic trap at a temperature ~ 200 μK . The oscillation frequency of the atoms along the longitudinal axis of the trap is $\omega_z/2\pi = 10.3$ Hz. For the results presented here, the transverse frequencies $\omega_\perp/2\pi$ have been varied between 170 and 210 Hz by adjusting the bias field at the center of the trap [15].

The experimental sequence consists of four steps: (i) condensation *via* evaporative cooling, (ii) vortex nucleation, (iii) excitation and evolution of the quadrupolar modes, and (iv) characterization using absorption imaging after a time-of-flight (TOF) expansion of $T_{\text{tof}} = 25$ ms. The probe laser for the imaging propagates along the z axis, and the image gives the transverse xy distribution of atomic positions after the expansion. From each image we extract the temperature of the cloud, the size of the condensate in the xy plane, and the number of vortices which have been nucleated.

We evaporatively cool the atoms with a radio-frequency sweep. The condensation threshold is reached at 550 nK. We continue the evaporative cooling to a temperature below 80 nK at which point approximately 3×10^5 atoms are left in the condensate. This number is evaluated from the size of the condensate after expansion, assuming an initial Thomas-Fermi distribution [16].

After the end of the cooling phase we switch on the stirring laser beam, which is parallel with the long axis of the condensate. The central position of this beam is varied in time with respect to the $x = y = 0$ axis by two acousto-optic modulators. This temporal variation and the stirring light intensity are chosen such that the stirring laser creates on the trapped atoms a dipole potential which is well approximated by $M\omega_\perp^2(\epsilon_X X^2 + \epsilon_Y Y^2)/2$

with $\epsilon_X = 0.05$ and $\epsilon_Y = 0.15$. The X, Y basis rotates at constant angular frequency Ω with respect to the fixed x, y basis. The stirring phase lasts 900 ms which is well beyond the typical vortex nucleation time found experimentally to be about 450 ms [17]. During this phase the evaporation frequency is raised to a relatively large value (magnetic well depth equal to 2 μK) in order not to perturb the nucleation process, and we observe a slight heating of the cloud with a final temperature of 130 (± 50) nK.

At the end of the vortex nucleation phase we excite a quadrupolar oscillation using the dipole potential created by the stirring laser now on a fixed basis ($X, Y = x, y$) and with a 10 times larger intensity. This potential acts on the atoms for a 0.3 ms duration, which is short compared to the transverse oscillation period. The potential created can be decomposed into (i) a part proportional to $x^2 - y^2$, which excites the transverse quadrupole motion of the condensate, and (ii) a part proportional to $x^2 + y^2$ which excites the transverse $m = 0$ breathing mode which is not relevant for the present study [18].

The transverse quadrupolar mode excited is a linear superposition of the $m = \pm 2$ modes. The lift of degeneracy between the frequencies of these two modes causes a precession of the eigenaxes of the quadrupole mode at an angular frequency given by $\dot{\theta} = (\omega_+ - \omega_-)/2|m| = (\omega_+ - \omega_-)/4$. Therefore the measurement of θ together with the size of the condensate gives access to L_z .

To determine $\dot{\theta}$ we let the atomic cloud oscillate freely in the magnetic trap for an adjustable period τ (between 0 and 8 ms) after the quadrupole excitation. We then perform the TOF + absorption imaging sequence, and we analyze the images of the condensate using a Thomas-Fermi-type distribution [19] as a fit function, with an adjustable ellipticity and adjustable axes in the xy plane.

A typical result is shown in Fig. 1. For this measurement the measured number of atoms was $3.7 (\pm 1.1) \times 10^5$. The transverse frequency $\omega_\perp/2\pi$ equals 171 Hz, and the threshold frequency $\Omega_c/2\pi$ for nucleating a vortex is 115 Hz. The sequences of pictures [Figs. 1(a)–1(c) and Fig. 1(d)–1(f)] correspond to $\tau = 1, 3,$ and 5 ms for which the ellipticity in the xy plane is maximum. Figures 1(a)–1(c) have been taken after stirring the condensate at a frequency $\Omega/2\pi = 114$ Hz. Since $\Omega < \Omega_c$, no

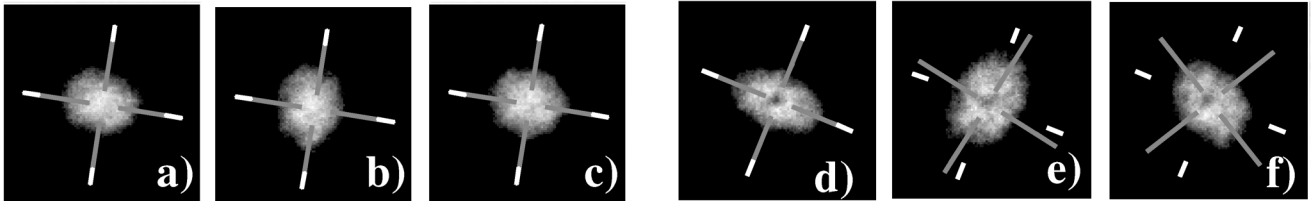


FIG. 1. Transverse oscillations of a stirred condensate with $N = 3.7 (\pm 1.1) \times 10^5$ atoms and $\omega_\perp/2\pi = 171$ Hz. For (a)–(c) the stirring frequency is $\Omega/2\pi = 114$ Hz, below the vortex nucleation threshold $\Omega_c/2\pi = 115$ Hz. For (d)–(f) $\Omega/2\pi = 120$ Hz. For (a),(d) $\tau = 1$ ms; (b),(e) $\tau = 3$ ms; (c),(f) $\tau = 5$ ms. The fixed axes indicate the excitation basis and the rotating ones indicate the condensate axes. A single vortex is visible at the center of the condensate in (d)–(f).

evidence for a vortex (which would appear as a density dip at the center of the condensate) is found in the corresponding images. The quadrupole oscillation is identical to the one found in the absence of the vortex nucleation phase. Its frequency 250 Hz (± 3 Hz) is in good agreement with the value $\sqrt{2}(\omega_{\perp}/2\pi)$ expected for a zero temperature condensate in the Thomas-Fermi limit [18].

For a stirring frequency $\Omega/2\pi = 120$ Hz for which a vortex is systematically nucleated at the center of the condensate, the behavior of the system is dramatically different. The axes of the quadrupole oscillation precess, as can be seen in the sequence of pictures [Figs. 1(d)–1(f)]. The precession rate θ , obtained from the analysis of several sequences of images taken every 0.5 ms, is $5.9(\pm 0.2)$ degrees per millisecond [i.e., $(\omega_{+} - \omega_{-})/2\pi = 66$ Hz].

In order to deduce from this precession the value of L_z we must determine the *in situ* size r_{\perp} of the condensate. The fit of the image of the condensate after expansion gives an average radius equal to $103 (\pm 6) \mu\text{m}$ (the radius is defined as the average distance from the center at which the Thomas-Fermi fit function vanishes). In our experimental conditions the time of flight corresponds to a dilatation of the transverse lengths by a factor $\sqrt{1 + \omega_{\perp}^2 T_{\text{tof}}^2} = 26.8$ [21,22], so that the radius of the condensate before time of flight is $R_{\perp} = 3.8 \mu\text{m}$. The Thomas-Fermi approximation yields $r_{\perp}^2 = 2R_{\perp}^2/7$ and we infer $L_z/\hbar = 1.2 (\pm 0.1)$. Note that the number of atoms is not needed in this determination of L_z .

We have performed similar experiments for several values of the stirring frequency Ω and of the oscillation frequency ω_{\perp} . For simplicity we have restricted our measurements to a single value of τ , corresponding to the third maximum in the temporal evolution of the ellipticity of the cloud (e.g., $\tau = 5$ ms for the parameters of Fig. 1). For each choice of Ω we measure θ , from which we deduce $\theta \approx \theta/\tau$, and the angular momentum.

The results are shown in Fig. 2 for the transverse frequency $\omega_{\perp}/2\pi = 175$ Hz. These data allow for a quantitative definition of the critical frequency Ω_c . This quantity was previously defined using a qualitative cri-

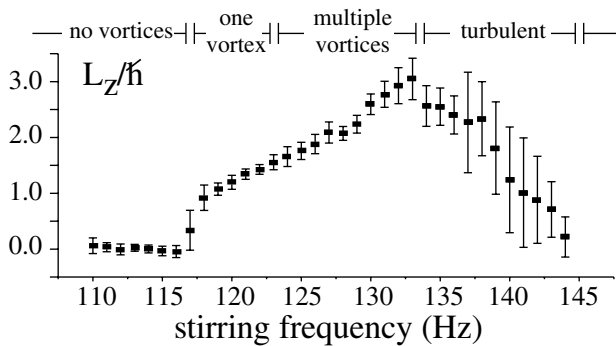


FIG. 2. Variation of the angular momentum deduced from (1) as a function of the stirring frequency Ω for $\omega_{\perp}/2\pi = 175$ Hz and $2.5 (\pm 0.6) \times 10^5$ atoms.

terion: the presence of a density dip at the center of the condensate. It can be defined now as the value for which L_z jumps from 0 to a value close to \hbar . The precision of this determination is of the order of 1 Hz, and it may be limited by the characteristic nucleation time (450 ms). For $\Omega \sim \Omega_c$ the large error bar in Fig. 2 reflects the large dispersion in the results for θ . This is illustrated more clearly in the histograms of Fig. 3 which give the value of L_z/\hbar for $\Omega/2\pi = 116, \dots, 118$ Hz.

For all transverse frequencies that we have used (between 170 and 220 Hz) we have found that $\Omega_c \approx 0.65\tilde{\omega}_{\perp}$, where $\tilde{\omega}_{\perp} = \omega_{\perp}[1 + (\epsilon_X + \epsilon_Y)/2]^{1/2}$ is the average transverse oscillation frequency in the presence of the stirring laser. The sensitivity of Ω_c to the atom number is very small: a change of N by a factor of 2 changes Ω_c by less than 5%. This is the reason for which the transition at Ω_c is so sharp, although the relative dispersion of the atom number is 40%. The measured value for Ω_c is notably larger (by $\sim 50\%$) than the predicted threshold above which the vortex state is energetically favored with respect to the nonvortex state [10,23–27]. A better account for the experimental result may be obtained by estimating the stirring frequency at which the energy barrier between these two states disappears [28–31].

To understand the details of Fig. 2, we recall that the angular momentum per particle in the condensate L_z depends in a nontrivial way on the configuration of the vortices. In particular, for a single vortex, L_z is equal to \hbar only when the vortex line coincides with the z axis. Otherwise L_z is strictly less than \hbar and decreases to 0 when the position of the vortex core reaches the edge of the condensate. Moreover, when \mathcal{N} vortices are present all corresponding to the same positive circulation h/M , the angular momentum per particle is lower than $\mathcal{N}\hbar$ unless all cores are superimposed along the z axis. This configuration, however, is unlikely to occur in our experiment since it is known that a vortex with a circulation $n\hbar/M$ where $n > 1$ is unstable [5,25–27,32].

In light of the above discussion, the jump in L_z from 0 to \hbar between 116 and 118 Hz corresponds to the transition from a zero vortex state to a state with a single, well centered vortex. This is confirmed by observing that the

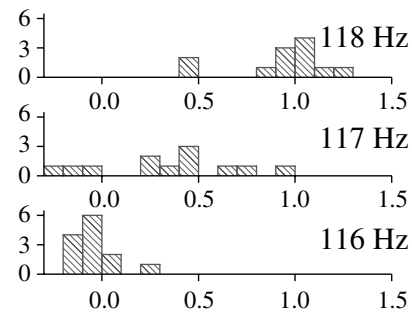


FIG. 3. Distribution of the values for L_z/\hbar for a stirring frequency $\Omega/2\pi = 116, \dots, 118$ Hz (same data as for Fig. 2).

vortex core nucleated at $\Omega/2\pi = 117$ Hz appears at the edge while the one nucleated at 118 Hz is on the center of the condensate after the time-of-flight expansion. As we increase the stirring frequency beyond 118 Hz L_z increases above \hbar , which according to the previous discussion should correspond to the entry of other vortices. On the time-of-flight images, multiple vortex structures are clearly apparent above $\Omega/2\pi = 124$ Hz. As the stirring frequency is varied from 120 to 124 Hz, although only one vortex is clearly visible, we observe that the deviation of its position with respect to the center of the condensate increases. This may be explained by the presence of a second vortex at the edge of the cloud where the density is too low for an unambiguous detection.

Between 118 and 133 Hz we observe a monotonic increase in the number of vortices nucleated from 1 to 5. The corresponding value for L_z varies from \hbar to a value smaller than $5\hbar$, as a consequence of the separation of the cores. The fact that the angular momentum increases continuously and exhibits no subsequent steps beyond the first probably reflects the smooth variation of the vortex core positions with Ω .

Another remarkable feature appearing in Fig. 2 is that for stirring frequencies between 133 and 145 Hz the precession rate decreases with Ω and the vortex lattice contrast “blurs” into a “turbulent” structure reported previously [13]. When the stirring frequency is $\Omega/2\pi = 145$ Hz we find no precession of the quadrupolar oscillation eigenaxes, and the atomic cloud appears to be unperturbed by the nucleation sequence. Moreover, the quadrupole and monopole oscillation frequencies are $256 (\pm 1)$ Hz, and $350 (\pm 1)$ Hz, respectively, which is very close to what is expected for a zero temperature condensate at rest, i.e., $\sqrt{2}\omega_\perp$ and $2\omega_\perp$ with $\omega_\perp/2\pi = 175$ Hz.

To summarize we have presented in this paper a direct measurement of the angular momentum of a Bose-Einstein condensate after it has been stirred at a given frequency Ω . Using only macroscopic quantities, namely, the precession angle and the spatial extension of the condensate, we have access to a microscopic value $\sim \hbar$ of the angular momentum per particle. This measurement relies on (1) which is valid only for a pure superfluid in the hydrodynamic regime [8]. In particular, it neglects the role of the thermal component, and it may not apply to the gas in the turbulent regime whose structure may be more complex than a “normal” Bose-Einstein condensate. This measurement is analogous to the experiment performed by Vinen in which he detected a single quantum of circulation in rotating He II by studying the lift of degeneracy between two vibrational modes of a thin wire placed at the center of the rotating fluid [33]. Also the existence of the threshold Ω_c for the stirring frequency at which the angular momentum per particle jumps from 0 to \hbar is a direct manifestation of the superfluidity of the condensate, and finally this complements the result of [34], showing that an “object” moving

at a velocity below a critical value does not deposit any energy in a condensate.

We thank E. Akkermans, V. Bretin, Y. Castin, C. Cohen-Tannoudji, P. Fedichev, D. Guéry-Odelin, C. Salomon, G. Shlyapnikov, S. Stringari, and the ENS Laser cooling group for several helpful discussions and comments. This work was partially supported by CNRS, Collège de France, DRET, DRED, and EC (TMR network ERB FMRX-CT96-0002). This material is based upon work supported by the North Atlantic Treaty Organization under an NSF-NATO grant awarded to K. W.M. in 1999. Laboratoire Kastler Brossel is Unité de recherche de l’Ecole Normale Supérieure et de l’Université Pierre et Marie Curie, associée au CNRS.

Note added.—After this work was completed we became aware of an experiment similar to that of Fig. 1 by Haljan *et al.* [35].

-
- [1] M.H. Anderson *et al.*, *Science* **269**, 198 (1995).
 - [2] C.C. Bradley *et al.*, *Phys. Rev. Lett.* **75**, 1687 (1995).
 - [3] K.B. Davis *et al.*, *Phys. Rev. Lett.* **75**, 3969 (1995).
 - [4] D. Fried *et al.*, *Phys. Rev. Lett.* **81**, 3811 (1998).
 - [5] E.M. Lifshitz and L.P. Pitaevskii, *Statistical Physics* (Butterworth-Heinemann, Stoneham, MA, 1980), Chap. III, Pt. 2.
 - [6] R. J. Donnelly, *Quantized Vortices in Helium II* (Cambridge University, Cambridge, England, 1991).
 - [7] M. Tinkham, *Introduction to Superconductivity* (McGraw-Hill, New York, 1980).
 - [8] F. Zambelli and S. Stringari, *Phys. Rev. Lett.* **81**, 1754 (1998).
 - [9] R. Dodd *et al.*, *Phys. Rev. A* **56**, 587 (1997).
 - [10] S. Sinha, *Phys. Rev. A* **55**, 4325 (1997).
 - [11] A. Svidzinsky and A. Fetter, *Phys. Rev. A* **58**, 3168 (1998).
 - [12] M. Matthews *et al.*, *Phys. Rev. Lett.* **83**, 2498 (1999).
 - [13] K. W. Madison *et al.*, *Phys. Rev. Lett.* **84**, 806 (2000).
 - [14] K. W. Madison *et al.*, cond-mat/0004037.
 - [15] The measured residual asymmetry of the magnetic trap is $\omega_{x,y} = \omega_\perp (1 \pm 9 \times 10^{-3})$.
 - [16] J. Söding *et al.*, *Appl. Phys. B* **69**, 257 (1999).
 - [17] This procedure is slightly different from the one in [13], where the stirring beam was switched on during the evaporation ramp, before the condensation was reached. Both methods lead to similar results, in particular, for Ω_c . The method followed here gives a slightly better control of the number of atoms in the condensate.
 - [18] S. Stringari, *Phys. Rev. Lett.* **77**, 2360 (1996).
 - [19] We use the usual “inverted parabola” function [20] which is found to provide a good fit for the condensate image, except in the vicinity of the vortex core.
 - [20] For a review, see, e.g., F. Dalfovo *et al.*, *Rev. Mod. Phys.* **71**, 463 (1999).
 - [21] Y. Castin and R. Dum, *Phys. Rev. Lett.* **77**, 5315 (1996).
 - [22] Yu. Kagan, E. L. Surkov, and G. V. Shlyapnikov, *Phys. Rev. A* **55**, R18 (1997).
 - [23] G. Baym and C. J. Pethick, *Phys. Rev. Lett.* **76**, 6 (1996).

- [24] E. Lundh, C. J. Pethick, and H. Smith, *Phys. Rev. A* **55**, 2126 (1997).
- [25] A. Fetter, *J. Low. Temp. Phys.* **113**, 189 (1998).
- [26] Y. Castin and R. Dum, *Eur. Phys. J. D* **7**, 399 (1999).
- [27] D. L. Feder, C. W. Clark, and B. I. Schneider, *Phys. Rev. Lett.* **82**, 4956 (1999).
- [28] F. Dalfovo *et al.*, *Phys. Rev. A* **56**, 3840 (1997).
- [29] T. Isoshima and K. Machida, *Phys. Rev. A* **60**, 3313 (1999).
- [30] Y. Castin (private communication).
- [31] D. L. Feder, C. W. Clark, and B. I. Schneider, *Phys. Rev. A* **61**, 011601(R) (1999); (private communication).
- [32] D. Butts and D. Rokhsar, *Nature (London)* **397**, 327 (1999).
- [33] W. F. Vinen, *Nature (London)* **181**, 1524 (1958); *Proc. R. Soc. London A* **260**, 218 (1961).
- [34] C. Raman *et al.*, *Phys. Rev. Lett.* **83**, 2502 (1999); A. P. Chikkatur *et al.*, cond-mat/0003387.
- [35] P. Haljan *et al.*, QELS, May 7–12, postdeadline session.